Polaritonic gap-soliton propagation through a wide defect in a resonantly absorbing Bragg grating

Elena V. Kazantseva[1,2,*] and Andrei I. Maimistov[3,†]
[1]*Department of Mathematics, University of Arizona, 617 North Santa Rita Avenue, Tucson, Arizona 85721, USA*
[2]*Laboratoire de Mathematiques de l'INSA de Rouen, B.P. 8, 76131 Mont-Saint-Aignan Cedex, France*
[3]*Department of Solid State Physics and Nanostructures, Moscow Engineering Physics Institute, Moscow, 115409, Russia*
(Received 11 November 2008; published 10 March 2009)

The three types of defects—microcavity (linear media without resonant nanoparticles), groove (the defect span with reduced density of nanoparticles), and stripe (the defect with high density of resonant atoms)—are discussed here. The nonlinear polariton transmission, reflection, and trapping by defects in the resonantly absorbing Bragg grating (RABG) are demonstrated by numerical simulations. A geometric optics interpretation is proposed to estimate the solitary polaritonic wave velocity inside wide defects such as grooves and stripes when the reflection on the interface between the RABG and a defect is negligible. The values of solitary wave velocity calculated from geometric optics approximation gives a good agreement with the values computed numerically. It is shown that the electromagnetic field propagating through RABG can be captured inside the microcavity placed in the RABG.

DOI: 10.1103/PhysRevA.79.033812 PACS number(s): 42.65.Tg, 42.70.Qs, 42.50.Gy

I. INTRODUCTION

In the last few years an interest in an object between electronics and photonics has arisen. The new terms polaritonics and plasmonics have attracted attention of the scientists and engineers. The interest in polaritonics is in interaction of light with microstructured matter. Due to the prominent progress that has occurred in the past few years in fabrication of novel materials with engineered internal structure (photonic band-gap fibers, carbon nanotubes, and nanowires), there is a demand for the analysis of the phenomena that can arise due to the specific properties of these artificial materials.

The substantial achievements in the fabrication of periodic structures in different materials have attracted interest in metallic periodic structures such as metallic combs, periodic array of indentations [1], two-dimensional hole lattices [2] and one-dimensional groove arrays [3] machined into flat interfaces, conducting wire tailored with a periodic array of radial grooves [4], and even "superstructures of nanowires and nanoparticles connected by molecular springs" [5]. The objects of interest are waves resulting from the photon interaction with plasmonic oscillations in metal [6]. The theory of surface plasmonic polaritions on structured surfaces, as well as the recent advances in experimental studies is reported [7]. The relevant method for preparation of a dielectric structure with periodic thin films containing metallic nanoparticles or molecules could be electron (e)-beam deposition or layer-by-layer adsorption technique [8], which allows for the creation of nanometer-scale multilayered films.

The nonlinear periodic structure that is referred to as a resonantly absorbing Bragg grating (RABG) has been proposed and investigated in [9–11]. The RABG consists of linear homogeneous dielectric medium containing a thin-film array of resonant two-level atoms. It has been shown that the stable bright and dark gap solitons exist in such a periodic medium. The results of the theory are summarized in [12]. An alterative kind of RABG is a regular Bragg grating constructed from the thin dielectric films bearing the metallic nanoparticles separated by half-wavelength nonabsorbing dielectric layers [13]. The nonlinear plasmonic oscillations in the nanoparticles are governed by the cubic Duffing equation. The reduced Maxwell equations describe the ultrashort pulse propagation in this RABG. Solitary electromagnetic waves coupled with wave of media polarization, i.e., polaritonic solitary waves, were found. The robustness of these *polaritonic gap solitons* (PGSs) was demonstrated by numerical simulation [13–15].

Optical soliton scattering on the defects in lattices is an attractive problem of nonlinear optics. Paper [16] is devoted to trapping light in a nonuniform resonant structure by a defect that is created as a result of the inversion of the atomic population. Depending on the strength of the defect the pulse can either pass through it with small radiation losses or localize on the defect. The action of the second pulse could lead to depinning of the initial pulse or to trapping both of them in the defect. Trapping the Bragg solitons by a pair of the localized defects has been also demonstrated [17]. Thus, it would be very natural to consider the interaction of the PGSs with different types of the defects in the RABG, such as the absence of films containing resonant atoms in the grating or, oppositely, the conglutination of several films. The influence of all these effects, arising in the process of artificial media fabrication, can be crucial in material guiding properties.

A homogeneous span between two distributed Bragg mirrors is the effective laser microcavity in integrated optics [18,19] and nano-optics [20–22]. During the past few years, the persistent interest in the optical properties of these structures subsists. The review of the nonlinear properties of semiconductor microcavities can be found [23]. The quantum well that is grown inside the Bragg-mirror microcavity

*elena@math.arizona.edu
†maimistov@pico.mephi.ru

appears as the defect in a regular periodic structure. So, the array of quantum wells in the Bragg-mirror microcavity is tantamount to the wide defect in the regular grating. A similar statement is true also for the resonantly absorbing Bragg grating.

The RABG is a partial example of a new type of artificial media, which is termed as a metamaterial (see [24]). Metamaterials consist of subwavelength-sized structure unites, which are intended to exhibit novel electromagnetic properties such as negative refractive index. The artificial media can be structured or disordered. In the case of a regular Bragg grating the efficient interaction of light with matter is provided due to its construction, such that the characteristic period of the media, which is akin to the lattice spacing, is of the same order as the radiation wavelength. The Bragg grating is a very fruitful and, at the same time, a well-explored model that can be applied to interpret structured metamaterials. The advantage here is that there is no need to introduce effective media with phenomenological permittivity ϵ and permeability μ. All electromagnetic parameters appear naturally from the model. The Bragg grating for the optical range of the waves is an analog of the crystal structure for x rays. Strong light-matter interaction can be observed when the radiation wavelength matches the lattice spacing.

In this paper we will discuss the three types of (wide) defect, which will be referred to as microcavity, groove, and stripe. Specification of these terms will be done below. We perform a numerical simulation of the coupled solitary waves, which interact resonantly with a medium consisting of dielectric layers alternating with thin films with nanoparticles (or quantum dots, nanoaggregates with nonlinear dielectric properties) [13]. Due to the Bragg resonance condition a weak electromagnetic pulse cannot propagate in the RABG, whereas the moving polaritonic gap soliton [13–15] is able to reach the inner defect.

II. MODEL DESCRIPTION

The model of the polaritonic wave propagating in resonantly absorbing Bragg grating is presented in detail in [13]. To take a look at the defects of RABG we generalize this model by including the indicator function $\gamma(\zeta)$, which takes into account an inhomogeneity in nanoparticle density. The indicator function is equal to the ratio of the nanoparticle density in the defect region per nanoparticle density in the regular region. The normalized form of the model equations becomes

$$i\left(\frac{\partial}{\partial\zeta}+\frac{\partial}{\partial\tau}\right)e_1+\delta e_1=-\gamma(\zeta)p,$$

$$i\left(\frac{\partial}{\partial\zeta}-\frac{\partial}{\partial\tau}\right)e_2-\delta e_2=+\gamma(\zeta)p,$$

$$i\frac{\partial}{\partial\tau}p+\Delta p+\mu|p|^2p=-(e_1+e_2). \tag{1}$$

Normalized spatial and time variables are denoted as $\zeta=(\omega_p/2c)x$ and $\tau=\omega_p t/2$, respectively, and ω_p is the plasma frequency. The variables $e_1=A/A_0$ and $e_2=B/A_0$ are normalized slowly varying envelopes of electric component of electromagnetic field, which propagate in the forward A and backward B directions. Also, $p=(4\pi\omega_0/\omega_p A_0)P$ is the slowly varying envelope of the polarization, which is determined by an array of thin films containing resonant nanoparticles. Here $\Delta=2(\omega_d-\omega_0)/\omega_p$ is the detuning of a nanoparticle's resonance frequency, i.e., a frequency of dimensional quantization of nanoparticles, ω_d, from the carrier wave frequency ω_0. $\delta=2(c/\omega_p)\Delta q_0$ with $\Delta q_0=q_0-2\pi/a$, $q_0=\omega_0/c$ is wave vector in the host media, and $\mu=(3k\omega_p/16\pi^2\omega_0^3)A_0^2$ is a dimensionless coefficient of anharmonicity which can be adjusted by variation in the normalization amplitude A_0. In following the parameter μ is set to 1. The total field acting on resonant nanoparticles is the sum of e_1 and e_2 [13].

FIG. 1. Distribution of nanoparticles density in (a) RABG microcavity $\gamma(\zeta)=0$, (b) RABG wide groove defect $\gamma(\zeta)<1$, and (c) RABG wide stripe defect $\gamma(\zeta)>1$.

Regular RABG is produced from thin layers with equal concentration of nanoparticles. For this reason we put $\gamma=1$ in the regular grating. The lattice defect is regarded as a span with alternative nanoparticles concentration (see Fig. 1). The region with $\gamma<1$ will be termed as the groove defect. The region where $(\gamma>1)$ will be denoted as the stripe defect. If the defect size is much larger than the solitary wave width, we will define that as a wide defect. Otherwise, the defect is considered to be narrow.

The solitary wave solution (i.e., the polaritonic gap soliton) corresponding to regular RABG has been found and discussed in [13,14]. When $\gamma(\zeta)$ is constant it reads as

$$e_1(\eta)=-0.5(1+\alpha)f(\eta)\exp\{i\delta\tau\},$$

$$e_2(\eta)=-0.5(1-\alpha)f(\eta)\exp\{i\delta\tau\},$$

$$p(\eta)=q(\eta)\exp\{i\delta\tau\}, \tag{2}$$

where $\eta=\tau-\alpha\zeta$, $\beta=2\gamma/(\alpha^2-1)$, and $\alpha>1$ is a free parameter defining the solitary wave group velocity. The auxiliary functions $f=u\exp\{i\varphi\}$ and $q=r\exp\{i\psi\}$ are defined through the following amplitudes:

$$u^2(\eta)=4\sqrt{\beta}\beta\cosh^{-1}[2\sqrt{\beta}(\eta-\eta_0)],$$

$$r^2(\eta)=4\beta\cosh^{-1}[2\sqrt{\beta}(\eta-\eta_0)], \tag{3}$$

and phases

$$\varphi(\eta)=\varphi_0\pm\arctan\tanh[\sqrt{\beta}(\eta-\eta_0)],$$

$$\psi(\eta)=\psi_0\pm 3\arctan\tanh[\sqrt{\beta}(\eta-\eta_0)]. \tag{4}$$

The initial phases are set in such way that $\varphi_0-\psi_0=\pi/2$ at $\eta\to-\infty$. In Eqs. (3) and (4) the parameter η_0 is an integration constant that indicates the initial pulse position.

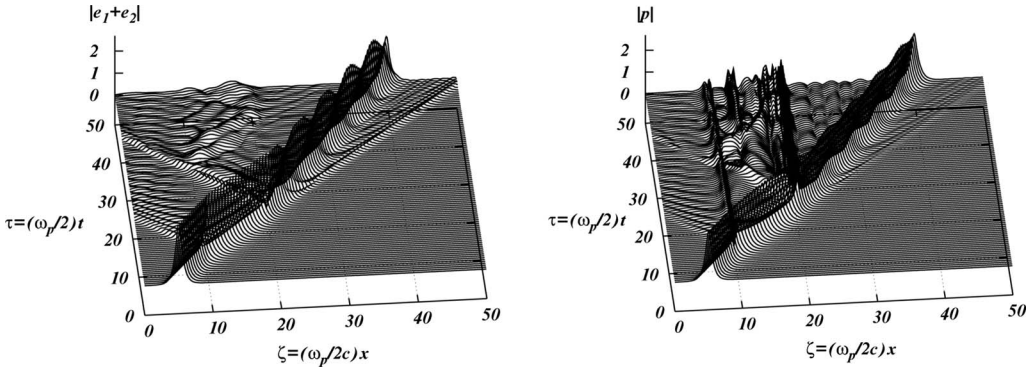

FIG. 2. Polaritonic gap-soliton ($\alpha=1.5$) interaction with wide groove with concentration determined by $\gamma=0.1$ at $(10<\zeta<20)$. The total electric field e_1+e_2 in units of $(A+B)/A_0$ and the polarization p in units of $(4\pi\omega_0/\omega_p A_0)P$ are represented versus temporal $\tau=\omega_p t/2$ and spatial $\zeta=(\omega_p/2c)x$ variables.

III. POLARITONIC GAP SOLITONS IN RABG: NUMERICAL SIMULATION

The nonlinear polaritonic wave (2) propagates through the ideal RABG without radiation loss or change in the initial shape. It should be noted that passing through the RABG is not allowed for linear waves due to the band gap. For this reason we use solution (2) as the initial configuration for our numerical simulation of the solitary wave propagation through the defect span in RABG (Fig. 1).

In all the following figures, which illustrate the results of numerical simulations, the wide defect is represented by the span with indicator function $\gamma\neq 1$. The left part of these pictures illustrates the evolution of the total electromagnetic field (e_1+e_2) and the right part represents the evolution of the polarization component p.

Considering the groove (i.e., the region with decreased concentration of resonant nanoparticles) one can see (Fig. 2) that part of incident pulse energy is expended for excitation of the plasmonic oscillations in the groove. Hence, the total electromagnetic field in cavity decreases (compared to the microcavity case).

Part of the polaritonic gap-soliton energy lost after passage through the cavity is spent in the generation of the periodic localized polarization modes, which can be seen at right of Fig. 2. These bright spots form a periodic pattern and are the result of reflection between a moving solitary pulse and the edge of the defect. We observed more pronounced periodic patterns for the polarization together with backward and forward waves (in total field they cancel each other due to interference) for the narrow defect (defect width is less than the PGS width).

Reducing the density gradient between the defect span and the regular grating results in drop of the radiation losses inside the groove-type defect ($\gamma=0.25, \gamma=0.5$). Linear polaritonic waves, which are trapped inside the groove, remain conspicuous. In case when the concentration of nanoparticles in the groove is half of the regular concentration, the polaritonic wave refraction at the fringes of the groove decreases and localization of the plasmonic modes tends to occur close to the fringes of the grove.

As follows from Eq. (2), and the definition of the variable η, the solitary wave velocity is controlled by parameter α. Increasing the value of α decreases the PGS velocity. A slow solitary wave interacts with defects more effectively. Systematic simulations have shown that in the case of a groove the slow PGS transfers more energy to plasmonic oscillations localized inside the defect and on the edges (see Figs. 3 and 4). The transmitted wave is almost negligible if the initial pulse has small velocity (see Fig. 4 for example).

Another type of the wide defect is a stripe of an optically denser medium. Provided that the nanoparticle density in the stripe is not too high ($\gamma=1.5$), the solitary polaritonic wave undergoes small losses of energy on the boundaries and the localization of polarization modes occurs only on the fringes of the stripe (Fig. 5). In this picture it is seen that almost all

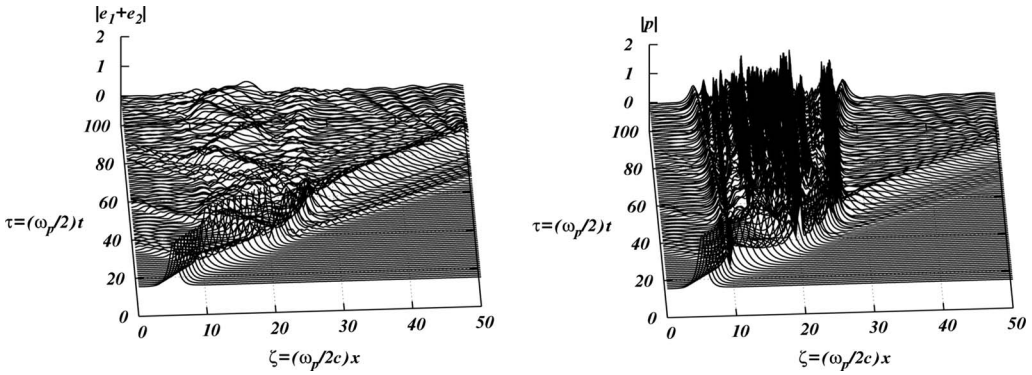

FIG. 3. Polaritonic gap-soliton ($\alpha=2$) interaction with wide groove with concentration determined by $\gamma=0.1$ at $(10<\zeta<20)$.

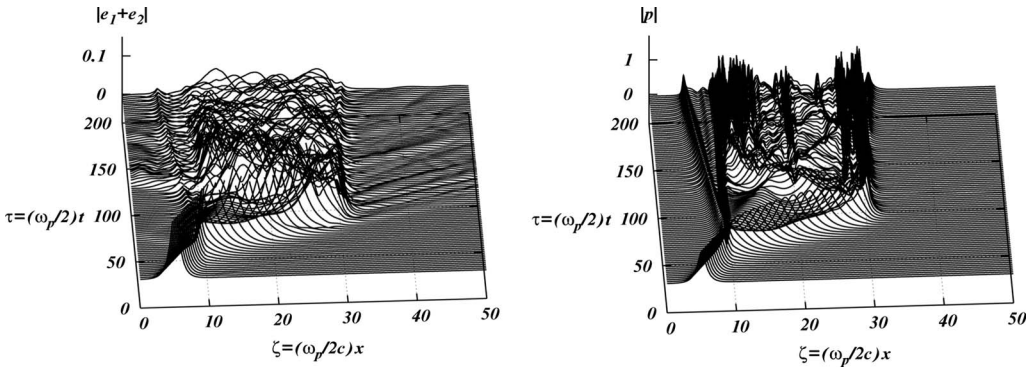

FIG. 4. Polaritonic gap-soliton ($\alpha=7$) interaction with wide groove with concentration determined by $\gamma=0.1$ at $(10<\zeta<30)$.

the energy of the electromagnetic wave remains in the transmitted pulse and less than half of the energy of the polaritonic wave transfers into the localized mode. The reflected wave is very weak.

In comparison to the groove-type defect almost no radiation remains inside the stripe defect after PGS passes this defect (compare, for example, Figs. 2 and 5). The localized polarization wave on the edges of the stripe-type defect emerges after the pulse hits the boundary between the normal RABG and the defect. Increasing the atomic density inside the stripe defect results in PGS dissipation with the appearance of the reflected backward waves. Some parts of the incident pulse create a trapped plasmonic mode and the rest of the pulse transfers forward after being converted into a solitary wave with smaller amplitude. With an increase in density of the resonant nanoparticles inside the defect, e.g., $\gamma=5$, the initial PGS is not powerful enough to survive in the dense defect and most of its electromagnetic component reflects backward. Also, a high energetic plasmonic mode locking with forepart of the stripe appears. Part of the radiation passes through the stripe defect in the RABG. In the case of narrow stripe of a dense material, the intensity of the transmitted pulse is higher and the pulse is more localized as compared with the pulse transmitted through the wide stripe with the same density. The polarization mode is defined only by the lower fringe reflection and it seems that it does not change with variation of the stripe width.

IV. GEOMETRIC OPTICS INTERPRETATION OF GAP-SOLITON REFRACTION

One could probably notice that the soliton trajectory in Figs. 2–5 reminds one of the light ray refracting at the boundaries of dielectric layers having different refractive indices. In optics, the continuity of the electric and magnetic fields leads to Fresnel relations and Snell's laws. The electric fields e_1 and e_2 are also continuous in the model under consideration. To show this we present variables [15] $f_s=e_1+e_2$ and $f_a=e_1-e_2$, then the first two equations of Eq. (1) become

$$\frac{\partial f_s}{\partial \zeta}+\frac{\partial f_a}{\partial \tau}=0,$$

$$\frac{\partial f_a}{\partial \zeta}+\frac{\partial f_s}{\partial \tau}=2i\gamma p. \tag{5}$$

Here $\delta=0$ is supposed for simplicity (continuity of the fields does not depend on detuning δ). Let us consider the sharp interface at $\zeta=0$ separating the gratings with γ_1 and γ_2 and a small neighborhood around this interface $(-\delta\zeta,+\delta\zeta)$. Integration of Eq. (5) over this neighborhood gives the following expressions:

$$f_s(\delta\zeta)-f_s(-\delta\zeta)+\delta\zeta\left(\frac{\partial f_a(\delta\zeta/2)}{\partial\tau}-\frac{\partial f_a(-\delta\zeta/2)}{\partial\tau}\right)=0,$$

$$f_a(\delta\zeta)-f_a(-\delta\zeta)+\delta\zeta\left[\frac{\partial f_s(\delta\zeta/2)}{\partial\tau}-\frac{\partial f_s(-\delta\zeta/2)}{\partial\tau}\right]$$
$$=-2i\delta\zeta[\gamma_2 p(\delta\zeta/2)-\gamma_1 p(-\delta\zeta/2)]. \tag{6}$$

By tending the transition layer thickness $2\delta\zeta$ to zero we obtain

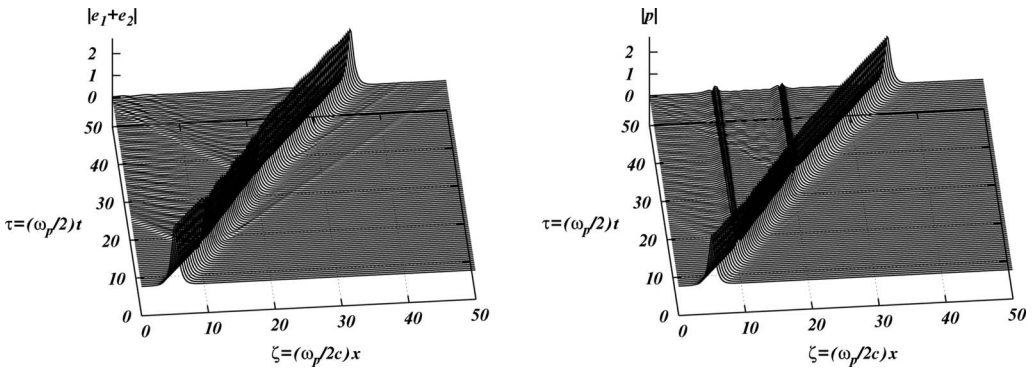

FIG. 5. Polaritonic gap-soliton ($\alpha=1.5$) transmission through the wide stripe with $\gamma=1.5$ at $(10<\zeta<20)$.

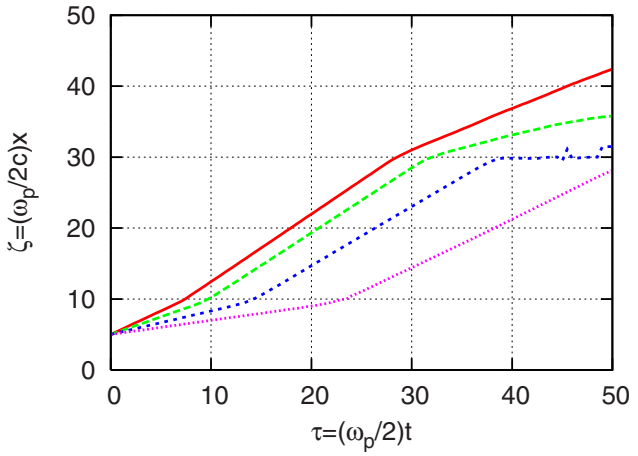

FIG. 6. (Color online) Propagation of a steady-state pulse through the wide groove with oscillator density $\gamma=0.1$ at $10<\zeta<30$ in the Bragg grating. The amplitudes of the pulses are different and defined by α: $\alpha=1.5$ (red solid curve), $\alpha=2$ (green dashed curve), $\alpha=3$ (blue short dotted curve), and $\alpha=5$ (pink dotted curve).

$$f_s(0-) = f_s(0+), \quad f_a(0-) = f_a(0+),$$

where $f_{a,s}(0\pm)=\lim_{\epsilon\to 0} f_{a,s}(0\pm\epsilon)$. This implies the continuity of the electric field on the interface, i.e.,

$$e_1(0-) = e_1(0+), \quad e_2(0-) = e_2(0+). \tag{7}$$

These expressions allow us to estimate the change in the PGS velocity after penetration into the defect with different oscillator densities. However, it is important to keep in mind that the electric fields in Eq. (7) include the transmitted PGS as well as the radiation reflected at the boundaries. We neglect the radiated and reflected parts and assume that the electric field of the incident solitary wave coincides with electric field of the PGS. From substitution of the solitary wave solutions (2) for the PGS in media with different densities, γ_1 and γ_2, into the continuity condition (7) it follows that the characteristic parameters, β, which depend on γ, for the PGS in different media are equal. Hence, we see that

$$\beta(\gamma_1) = \beta(\gamma_2).$$

Thus, we obtain the following expression connecting the soliton group velocities in media with different densities γ_1 and γ_2:

$$\alpha_2^2 = 1 + \frac{\gamma_2}{\gamma_1}(\alpha_1^2 - 1). \tag{8}$$

Neglecting the radiation part presumes that the accurate result can be obtained when the radiation is weak. The numerical results show that the small amount of radiation is shed after interaction of the powerful PGS with defect. Consequently, the best approximation for the velocity of the PGS formed inside the homogeneous defect could be expected for the initial powerful pulses with small α. We tested this simple approximation to estimate the PGS velocity in a groove with oscillator density $\gamma=0.1$ and in a stripe with $\gamma=1.5$. The trajectories of the total electric field component for

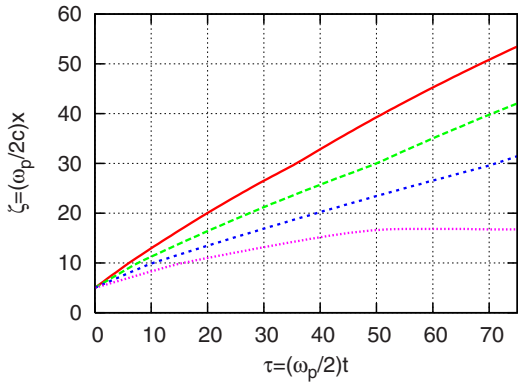

FIG. 7. (Color online) Trajectory of a PGS propagating through the Bragg grating with stripe defect having oscillator density $\gamma=1.5$ at $10<\zeta<30$. The amplitudes of the pulses are different and defined by α: $\alpha=1.2$ (red solid curve), $\alpha=1.5$ (green dashed curve), $\alpha=2$ (blue short dotted curve), and $\alpha=3$ (pink dotted curve).

the PGS with different velocities ($\alpha=1.5,2,3,5$) are represented in (Fig. 6) for the groove. We compare the values of the solitary wave velocities in the groove from these numerically obtained plots with our approximative formula (8). As expected the agreement between the numerical simulation and approximation is very good for small initial velocity $\alpha=1.5$: the value of the numerically obtained PGS group velocity $\alpha_{\text{num}}=1.06$ exactly coincides with approximate value $\alpha_{\text{approx}}=1.06$ (at the exit into the regular grating $\alpha_{\text{num}}=1.75$). Increasing the initial velocity, $\alpha_0=2$, results in small difference between numerical and analytical results: $\alpha_{\text{num}}=1.12$ and $\alpha_{\text{approx}}=1.14$. For $\alpha_0=3$ the imprecision of the approximation used becomes noticeable (about 10%): $\alpha_{\text{num}}=1.2$ and $\alpha_{\text{approx}}=1.34$.

The trajectories of the total electric field component for the PGS with different velocities corresponding to $\alpha=1.2$, 1.5, 2, and 3 are represented (Fig. 7) for the stripe-type defect. Comparison to the solitary wave velocities in the defect obtained from approximation (8) with numerically obtained values gives less accurate results relative to the groove-type defect. For example, if the PGS with $\alpha_0=1.2$ penetrates into the stripe then the numerically obtained value of the PGS velocity inside the stripe corresponds to $\alpha_{\text{num}}=1.5$ and the approximation gives $\alpha_{\text{approx}}=1.288$. For the PGS with $\alpha_0=1.5$ the values of the parameter α inside the stripe are $\alpha_{\text{num}}=2.1$ and $\alpha_{\text{approx}}=1.695$.

When the PGS penetrates into the media with smaller oscillator density (groove defect), it drops some radiation on the interface; however, the energy remaining enough to transform into the soliton with parameters corresponds to the low-density media. Oppositely, when the PGS penetrates into the media with higher oscillator density (stripe defect), it drops some radiation on the interface; however, the energy remaining is not enough for transformation into the soliton and the pulse trajectory is not a straight line as it should be for the soliton. For this reason, the quasioptical approximation is not as accurate for the description of the stripe-type defect.

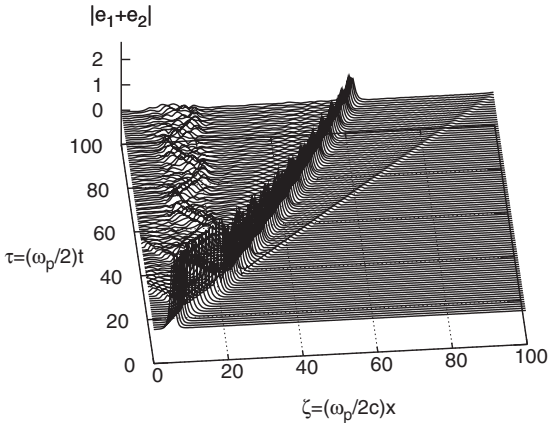

FIG. 8. An example of PGS ($\alpha=1.5$) evolution in the RABG with microcavity.

V. TRAPPING OF THE POLARITONIC GAP SOLITON BY MICROCAVITY

We consider microcavity, i.e., wide defect, which does not include the resonant nanoparticles, as the special example of the wide defect in the RABG. At the front of the interface of the defect, as Fig. 8 demonstrates, the incident polaritonic gap soliton transforms to the electromagnetic pulse that propagates in a linear medium until it crosses the second interface of the microcavity. (Inside the defect the pulse velocity coincides with velocity of linear wave.) Nearly all the energy of the incident polaritonic gap soliton transfers to this linear wave. Having traversed the cavity, the pulse sheds radiation on the second edge of the defect. Since the reflected pulse has a small amplitude (less 0.2–0.4 of the incident pulse amplitude), it transforms into linear waves, which remain trapped in the cavity as they cannot further propagate in the RABG. The pulse refracted on the second interface restores the plasmonic wave, so that a nonlinear solitary polaritonic wave arises again, but with smaller energy.

It is relevant to mention that the characteristic of the refracted pulse passing through microcavity corresponds to light ray passing the dielectric layer according to geometric optics laws. In the microcavity the velocities of all the pulses are the same and equal to 1 in normalized units. They do not depend on the initial α. Slow PGS (corresponding to $\alpha=7$ in Fig. 9) can be trapped by microcavity. Neither dispersion nor nonlinearity affects the pulse inside the microcavity.

The part of radiation from the PGS trapped inside the microcavity reflects at the boundary of the empty area and the distributed mirror. Every collision results in scattering of waves inside the cavity and after a few collisions the solitary wave is dissipated. Launching the PGS with even smaller velocity ($\alpha=10$ in Fig. 10) results in a more effective wave trapping inside the microcavity. Nevertheless, this regime of propagation turns out to be unstable and the solitary pulse eventually dissipates inside the microcavity. Beyond the microcavity there is virtually no radiation.

VI. CONCLUSION

In our consideration we applied the model of RABG to treat the propagation of the coupled electromagnetic wave and polarization—the polariton in the structured metamaterial. The solution corresponding to coupled light-matter steady-state wave (polaritonic gap soliton) for the regular RABG is adapted to the RABG with included extended homogeneous density defect. The transmission and scattering on the boundaries of the defected RABG were studied numerically for the three types of density defects. The interest here was to consider how the structural defects included in the ordered metamedia affected the light-matter wave propagation in the media. We assumed a normal incidence of the polaritonic gap soliton for the sake of simplicity.

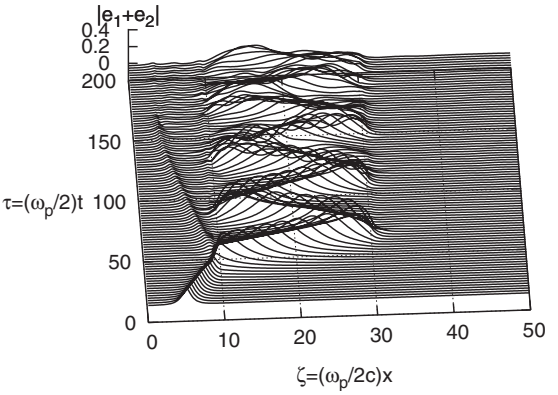

FIG. 9. A PGS with $\alpha=7$ is trapped in the microcavity ($\gamma=0$).

In particular the PGS launched at the interface of RABG with a groove-type defect, transmitted through this material, has considerable loss in both parts of the electromagnetic and polarization components inside this low-density defect. Some parts of the radiation remain localized on the groove boundaries. A geometric optics approximation used to estimate PGS velocity inside wide defect with low density proves to be very accurate when the radiation neglected in the approximation involving continuity of the fields at the boundary of two layers is weak.

The near-total reflection resulted in PGS collapse on the stripe defect with high oscillator density is demonstrated in numerical simulation. Generation of localized oscillations of polarization attends the solitary wave scattering on the defect. A stripe-type defect with high density of nanoparticles could serve as a guide for highly intensive polarization mode that propagates along the defect edge.

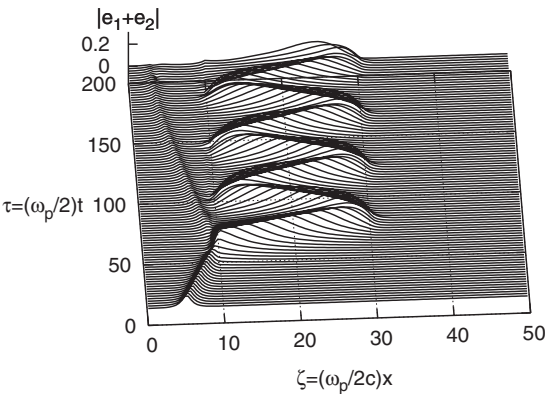

FIG. 10. Slow PGS ($\alpha=10$) trapping in the microcavity ($\gamma=0$).

Slow PGS trapping was demonstrated for the microcavity placed into RABG. The pulse exhibited multiple reflections from the boundary between the microcavity and RABG. Due to the imperfect reflection some parts of the trapped pulse energy are lost. This determines the lifetime of the pulse inside the microcavity. In this paper we considered the normal incidence of the soliton; however, oblique incidence could be a more preferable way to trap the pulse inside the microcavity.

ACKNOWLEDGMENTS

We are grateful to Professor Ildar Gabitov and Dr. Alexander Korotkevich for enlightening discussions. The authors thank Bridget Kennedy for her kind help to improve the text of the paper. The authors appreciate the hospitality and support of the Department of Mathematics at the University of Arizona. This work was funded by the State of Arizona Grant TRIF-Proposition No. 301 and in part by the Russian Foundation for Basic Research (Grant No. 06-02-16406).

[1] F. Lopez-Tejeira *et al.*, Nat. Phys. **3**, 324 (2007).
[2] J. B. Pendry, L. Martin-Moreno, and F. J. Garcia-Vidal, Science **305**, 847 (2004).
[3] F. J. Garcia-Vidal, L. Martin-Moreno, and J. B. Pendry, J. Opt. A, Pure Appl. Opt. **7**, S97 (2005).
[4] S. A. Maier, S. R. Andrews, L. Martin-Moreno, and F. J. Garcia-Vidal, Phys. Rev. Lett. **97**, 176805 (2006).
[5] J. Lee, P. Hernandez, J. Lee, A. O. Govorov, and N. A. Kotov, Nature Mater. **6**, 291 (2007).
[6] M. Ziman, *Principles of the Theory of Solids* (Cambridge University Press, Cambridge, England, 1979).
[7] A. V. Zayats, I. I. Smolyaninov, and A. A. Maradudin, Phys. Rep. **408**, 131 (2005).
[8] G. Decher, Science **277**, 1232 (1997).
[9] B. I. Mantsyzov and R. N. Kuzmin, Zh. Eksp. Teor. Fiz. **91**, 65 (1986) [Sov. Phys. JETP **64**, 37 (1986)].
[10] A. Kozhekin and G. Kurizki, Phys. Rev. Lett. **74**, 5020 (1995).
[11] B. I. Mantsyzov, JETP Lett. **82**, 253 (2005).
[12] G. Kurizki, A. E. Kozhekin, T. Opatrny, and B. A. Malomed, *Optical Solitons in Periodic Media with Resonant and Off-Resonant Nonlinearities*, in Progress in Optics, edited by E. Wolf (North Holland, Amsterdam, 2001), Vol. 42, pp. 93–146.
[13] I. R. Gabitov, A. O. Korotkevich, A. I. Maimistov, and J. B. McMahon, Appl. Phys. A: Mater. Sci. Process. **89**, 277 (2007).
[14] A. I. Maimistov, I. R. Gabitov, and A. O. Korotkevich, Quantum Electron. **37**, 549 (2007).
[15] I. R. Gabitov, A. O. Korotkevich, A. I. Maimistov, and J. B. McMahon, in *Dissipative Solitons: From Optics to Biology and Medicine*, Lecture Notes in Physics Vol. 751, edited by N. Akhmediev and A. Ankievich (Springer, Berlin, 2008), pp. 337–360.
[16] I. V. Mel'nikov, J. S. Aitchison, and B. I. Mantsyzov, Opt. Lett. **29**, 289 (2004).
[17] P. Y. P. Chen, B. A. Malomed, and P. L. Chu, Phys. Rev. E **71**, 066601 (2005).
[18] A. Yariv and M. Nakamura, IEEE J. Quantum Electron. **13**, 233 (1977).
[19] C. Elachi and C. Yeh, J. Appl. Phys. **44**, 3146 (1973).
[20] A. V. Kavokin, M. A. Kaliteevski, and M. R. Vladimirova, Phys. Rev. B **54**, 1490 (1996).
[21] S. P. Kennedy and R. T. Phillips, J. Opt. Soc. Am. B **15**, 1610 (1998).
[22] M. Richard, J. Kasprzak, R. Romestain, R. André, and L. S. Dang, Phys. Rev. Lett. **94**, 187401 (2005).
[23] G. Khitrova, H. M. Gibbs, F. Jahnke, M. Kira, and S. W. Koch, Rev. Mod. Phys. **71**, 1591 (1999).
[24] E. Shamonina and L. Solymar, Metamaterials **1**, 12 (2007).